Control Theory Tech, Vol. 16, No. 2, pp. 133–144, May 2018

Control Theory and Technology

http://link.springer.com/journal/11768

Nonlinear robust control of a quadrotor helicopter with finite time convergence

Guozhou ZHENG, Bin XIAN†

School of Electrical and Information Engineering, Tianjin University, Tianjin 300072, China

Received 19 August 2016; revised 18 August 2017; accepted 10 November 2017

Abstract

In this paper, the control problem for a quadrotor helicopter which is subjected to modeling uncertainties and unknown external disturbance is investigated. A new nonlinear robust control strategy is proposed. First, a nonlinear complementary filter is developed to fuse the raw data from the onboard barometer and the accelerometer to decrease the negative effects from the noise associated with the low-cost onboard sensors Then the adaptive super-twisting methodology is combined with a backstepping method to formulate the nonlinear robust controller for the quadrotor's attitude angles and the altitude position. Lyapunov based stability analysis shows that finite time convergence is ensured for the closed-loop operation of the quadrotor's roll angle, pitch angle, row angle and the altitude position. Real-time flight experimental results, which are performed on a quadrotor flight testbed, are included to demonstrate the good control performance of the proposed control methodology.

Keywords: Quadrotor, nonlinear control, finite time convergence, real-time experiment

DOI https://doi.org/10.1007/s11768-018-6124-7

1 Introduction

The navigation and control of unmanned aerial vehicles (UAVs), also known as drones, has become an important research area over the past decades [1,2]. As a micro helicopter, the quadrotor UAV attracts great attention from military and civil applications due to its special advantages such as simple structure, vertical taking off and landing (VTOL), and rapid maneuvering. It has been widely used in a variety of situations including surveillance, fire flighting, environmental monitoring, etc. [3–5]. Comparing to the flapping-wing aircraft and other configurations, quadrotor UAV is simple in mechanism, and its four identical rotors are the only moving parts onboard. The simplicity in mechanism is a trade-off with the dependency of sophisticated flight controller [6, 7]. However, the quadrotor is a highly nonlinear and time-varying system, and it has

†Corresponding author.

E-mail: xbin@tju.edu.cn. Tel.: +86-22-27400897; fax: +86-22-27400897.

This work was supported by the Key Project of Tianjin Science and Technology Support Program (No. 15ZCZDGX00810), the Natural Science Foundation of Tianjin (No. 14JCZDJC31900), and the National Natural Science Foundation of China (Nos. 91748121, 90916004, 60804004).

an unstable open-loop dynamics [8]. Additionally, due to its small size and weight, the quadrotor is very sensitive to external aerodynamic disturbances such as wind gusts and ground effect. Therefore, the design of high-performance nonlinear control mechanisms for quadrotors in the presence of structural uncertainties and unknown external disturbances is still a challenging task.

To guarantee a safe and steady flight against external disturbances, various control methods have been developed for quadrotors in recent years. In [9], the authors developed an H_∞ based attitude controller for the quadrotor's attitude subsystem. In [10], the time-varying disturbance was treated as a new unknown state and estimated by an extended observer. Then, a sliding mode based feedback controller was employed for the attitude stabilization, and numerical simulation results were included. An integral sliding mode based robust controller is proposed for the control of a quadrotor in [11], though the proof of the stability and numerical simulation results were presented, the control gains were not very easy to be tuned. In [12], the authors developed a nonlinear robust attitude control algorithm for a quadrotor with uncertain dynamics by combing a PD controller with a robust compensator, and ultimately bounded attitude tracking result was proven. Based on these works in [12], the authors former extend the control strategy in [13], where both position and attitude controllers were developed, the tracking error were proven to be kept within a known neighborhood of the origin ultimately. A nonlinear robust adaptive was developed in [14] for a quadrotor with linear parameterized (LP) uncertain-ties and bounded disturbances, semiglobally asymptotic tracking of a time-varying position trajectory and yaw angle trajectory was proved via a Lyapunov-based stability analysis. In [15], authors designed an attitude controller by using exponential coordinates to avoid singuarlities, and trajectory linearization method was employed to facilitate the control design procedure.

Though a lot of controller have been developed for the control of quadrotors, most of them can not guarantee the convergence time for the quadrotor's outputs. The super twisting algorithm, which is a second order continuous sliding mode control technique that ensures robustness in the presence of the smooth matched disturbance with bounded gradient, is implemented for attitude control of a quadrotor in [16] with known knowledge of the boundary of the disturbance gradient.

Motivated by the control methodology presented in [17], we develop a new nonlinear robust controller for the quadrotor with the attitude angles and altitude position selected as the system's outputs. An adaptive super-twisting algorithm is combined with backstepping method to formulate the controller. The proposed controller does not require the exact knowledge of the boundary of the disturbance or its gradient. By using the super-twisting algorithm, the control inputs to the quadrotor suffers little from the chattering phenomenon, and the adaptive laws ensure that the control gains will be easy to be tuned. Lyapunov based stability analysis is employed to show that the closed-loop operation is stable, and the tracking errors converges to a neighborhood of the origin with finite convergence time. Moreover, to increase the measurement accuracy for the altitude channel where low-cost onboard sensor were very sensitive to noise, a nonlinear complementary filter is developed to fuse the raw data from the onboard accelerometer and barometer. The stability and convergence of the filter is also proven via Lyapunov based analysis. Real-time experimental results are implemented on a self-made quadrotor helicopter testbed, the results show that the proposed control strategy has achieved good control performance for the quadrotor.

Therefore, the contribution of the proposed design includes that: 1) a nonlinear complementary filter is designed to provide accurate estimation for the quadrotor helicopter's altitude based on raw data from the onboard low cost sensors; 2) the super-twisting based nonlinear controller can achieve finite time convergence of the attitude tracking error under the effects of unknown external disturbances without exact knowledge of the disturbances' upper bound; and 3) real-time flight experimental results have testified the good performance of the proposed methodology.

This paper is organized as follows: The dynamics model of the quadrotor helicopter and control objective are described in Section 2. Section 3 presents the design of the nonlinear complementary filter design for the altitude channel. Section 4 provides details of the control development and stability analysis. Real-time experimental results are included in Section 5 to validate the controller's performance. Finally, some conclusion remarks are included in Section 6.

2 Dynamic model of the quadrotor

The quadrotor UAV can be considered as a rigid body with 6 degree-of-freedom (DOF): three translational motions and three rotational motions As illustrated in Fig. 1, two frames are utilized to represent the motion of the quadrotor. Let $I = \{x_I, y_I, z_I\}$ denote the right-hand inertia reference frame, and $B = \{x_B, y_B, z_B\}$ denote the right-hand body-fixed reference frame. The altitude of the UAV with respect to I is denoted by $z(t) \in \mathbb{R}$, and Euler angle vector of the UAV with respect to I is denoted by $\eta(t) = [\phi(t)\ \ \theta(t)\ \ \psi(t)]^{\mathrm{T}} \in \mathbb{R}^3$ where $\phi(t)$, $\theta(t)$ and $\psi(t)$ are the quadrotor's roll angle, pitch angle, and yaw angle, respectively. The rotation matrix from B to I is presented as follows [18]:

$$R(\eta) = \begin{bmatrix} c\theta c\psi & -c\phi s\psi + s\phi s\theta c\psi & s\phi s\psi + c\phi s\theta c\psi \\ c\theta s\psi & c\phi c\psi + s\phi s\theta s\psi & -s\phi c\psi + c\phi s\theta s\psi \\ -s\theta & s\phi c\theta & c\phi c\theta \end{bmatrix}, \tag{1}$$

where $c(\cdot)$ is the abbreviation for $\cos(\cdot)$, and $s(\cdot)$ is the abbreviation for $\sin(\cdot)$. In Fig. 1, f_i for $i = 1, \dots, 4$, represents the independent thrust force generated by the four rotors of the quadrotor.

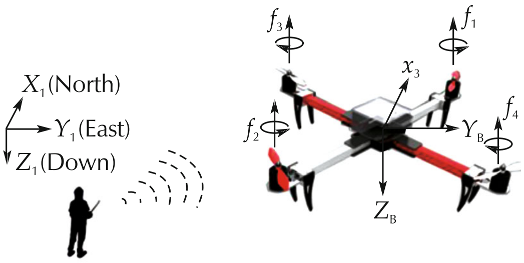

Fig. 1 Schematic of a quadrotor UAV.

The attitude dynamics of the quadrotor considered in this paper can be modeled via the following differential equations [18]:

$$\begin{cases} J\dot{\Omega} + \Omega \times (J\Omega) = \tau + d, \\ \dot{\eta} = \Phi(\eta)\Omega, \end{cases} \tag{2}$$

where $\Omega(t) = [p(t)\ \ q(t)\ \ r(t)]^{\mathrm{T}}$ represents the angular velocity vector of the quadrotor with respect to B, $\tau(t) = [\tau_\phi(t)\ \ \tau_\theta(t)\ \ \tau_\psi(t)]^{\mathrm{T}} \in \mathbb{R}^3$ denotes the control torque input vector, $d(t) = [d_\phi(t)\ \ d_\theta(t)\ \ d_\psi(t)]^{\mathrm{T}} \in \mathbb{R}^3$ is the unknown external disturbance moment vector. In (2), $J = \mathrm{diag}\{[J_\phi\ \ J_\theta\ \ J_\psi]\} \in \mathbb{R}^{3\times 3}$ denotes the inertia matrix with J_ϕ, J_θ, and J_ψ being some positive constants, the matrix $\Phi(\eta) \in \mathbb{R}^{3\times 3}$ represents the rotational velocity transfer matrix from B to I which has the following form [4]

$$\Phi(\eta) = \begin{bmatrix} 1 & s\phi s\theta/c\theta & c\phi s\phi/c\phi \\ 0 & c\phi & -s\phi \\ 0 & s\phi/c\theta & c\phi/c\theta \end{bmatrix}. \tag{3}$$

The following assumption will be employed in the subsequent control development.

Assumption 1 The disturbance term d and its time derivative $\dot{d}$ are bounded such that $\|d\|_\infty \leqslant \delta_1$, $\|\dot{d}\|_\infty \leqslant \delta_2$ where δ_1 and δ_2 are some unknown positive constants.

The dynamic model for the altitude channel of the quadrotor is shown as follows [18]:

$$m\ddot{z} = -u_{\mathrm{t}} \cos\phi \cos\theta + mg + d_{\mathrm{t}}, \tag{4}$$

where $m \in \mathbb{R}$ represents the mass of the quadrotor, $u_{\mathrm{t}} \in \mathbb{R}$ is the total thrust in the z-direction, g is the acceleration of gravity, and $d_{\mathrm{t}}(t) \in \mathbb{R}$ denotes the unknown external disturbance force in the z-direction. The following assumption will be utilized in the subsequent control development.

Assumption 2 The disturbance item d_{t} and its time derivative $\dot{d}_{\mathrm{t}}$ are bounded such that $\|d_{\mathrm{t}}\|_\infty \leqslant \delta_{z1}$, $\|\dot{d}_{\mathrm{t}}\|_\infty \leqslant \delta_{z2}$ where δ_{z1} and δ_{z2} are some unknown positive constants.

Assumption 3 The roll angle $\phi(t)$ and the pitch angle $\theta(t)$ satisfy the following inequalities:

$$\phi(t) \neq \pi/2, \quad \theta(t) \neq \pi/2. \tag{5}$$

This assumption has also been employed in [13].

The relationship between the control inputs $[\tau_\phi\ \tau_\theta\ \tau_\psi\ u_{\mathrm{t}}]^{\mathrm{T}}$ and the rotor thrusts force $[f_1\ \ f_2\ \ f_3\ \ f]^{\mathrm{T}}$ is given by

$$\begin{cases} \tau_\phi = l_{\mathrm{f}}(f_2 + f_3 - f_1 - f_4), \\ \tau_\theta = l_{\mathrm{f}}(f_1 + f_3 - f_2 - f_4), \\ \tau_\psi = p_{\mathrm{f}}(f_1 + f_2 - f_3 - f_4), \\ u_{\mathrm{t}} = f_1 + f_2 + f_3 + f_4, \end{cases} \tag{6}$$

where l_{f} is the distance from each rotor to the center of the quadrotor, and p_{f} is the force-to-moment scaling factor.

The main control objective is to design control inputs (τ, u_{t}) to drive the quadrotor's outputs $(\eta(t), z(t))$ to track some pre-defined reference trajectory $(\eta_{\mathrm{d}}(t), z_{\mathrm{d}}(t))$.

3 Nonlinear complementary filter for the altitude measurement

In this paper, two low cost and light weight onboard sensors are employed to provide altitude measurements for the quadrotor, the first one is the barometer, and the other one is the accelerometer. The onboard barometer can provide a rough relative altitude measurement with an accuracy of about ±0.5 m which is not good enough for accurate hovering control of the quadrotor, and the onboard accelerometer returns an acceleration measurement in the altitude direction which is characterized with high noise levels and biases. A nonlinear complementary filter is introduced to deal with the misalignment of the accelerometer axes and factitious placement failure as well as some other nonlinearities, thus good altitude estimation can be obtained via the raw outputs from the barometer and the accelerometer.

To implement the nonlinear altitude fusion algorithm, an altitude measurement dynamics model with consideration of the proposed nonlinearities is introduced as follows:

$$\ddot{z} = Y(PA_{\mathrm{m}} - Q) + g, \tag{7}$$

where $z(t)$ is defined in (4) and denotes the real altitude value of the quadrotor, $P \in \mathbb{R}^{3\times3}$ denote a matrix relevant to the misalignment of the sensor axes and measuring sensitivity differences among each axis, $Y = e_3^{\mathrm{T}}R \in \mathbb{R}^{1\times3}$ denotes the transpose of the third column of the rotation matrix R defined in (1), $Q \in \mathbb{R}^3$ denote the bias vector, and $A_{\mathrm{m}} \in \mathbb{R}^3$ denotes the outputs from the accelerometer.

Remark 1 In an ideal circumstance where the accelerometer's outputs reflect the real acceleration value of the quadrotor, P will equal to an identity matrix I_3, and Q will be a zero vector.

Assumption 4 The matrix P and Q in (7) are unknown constant terms such that $\dot{P} = 0_{3\times3}$, $\dot{Q} = 0_{3\times1}$. And the altitude channel is assumed to be measurable for low frequency such that $z_{\mathrm{m}}(t) \approx z(t)$ where $z_{\mathrm{m}}(t)$ denotes a reconstructed altitude measurement [22].

Let the auxiliary estimation errors $e_{\mathrm{m}}(t), \sigma_{\mathrm{m}}(t) \in \mathbb{R}$ be defined as follows:

$$\begin{cases} e_{\mathrm{m}} = z_{\mathrm{m}} - \hat{z}, \\ \sigma_{\mathrm{m}} = \dot{e}_{\mathrm{m}} + \lambda_z e_{\mathrm{m}}, \end{cases} \tag{8}$$

where $\hat{z}(t) \in \mathbb{R}$ is the output of the following nonlinear complementary filter, and λ_z is a positive constant. The nonlinear complementary filter for the altitude channel is designed as follows:

$$\begin{cases} \dot{\hat{z}} = \hat{v} + (\alpha_z + \lambda_z)e_{\mathrm{m}}, \\ \dot{\hat{v}} = Y(\hat{P}A_{\mathrm{m}} - \hat{Q}) + g + \alpha_z\lambda_z e_{\mathrm{m}}, \end{cases} \tag{9}$$

where α_z is a positive constant, $\hat{v}(t)$ denotes the estimation for the vertical speed. The adaptive laws of $\hat{P}(t)$ and $\hat{Q}(t)$ are designed as

$$\begin{cases} \dot{\hat{Q}} = -k_1\sigma_{\mathrm{m}}Y^{\mathrm{T}}, \\ \dot{\hat{P}} = k_2\sigma_{\mathrm{m}}(A_{\mathrm{m}}Y)^{\mathrm{T}}. \end{cases} \tag{10}$$

Let the auxiliary error signals $e_z(t) \in \mathbb{R}$, $\sigma_z \in \mathbb{R}$, $\tilde{P}(t) \in \mathbb{R}^{3\times3}$, and $\tilde{Q} \in \mathbb{R}^3$ be defined as follows:

$$\begin{cases} e_z = z - \hat{z}, \quad \sigma_z = \dot{e}_z + \lambda_z e_z, \\ \tilde{P} = P - \hat{P}, \quad \tilde{Q} = Q - \hat{Q}. \end{cases} \tag{11}$$

Taking Assumption 2 into account, (9) and (10) can be rewritten as

$$\begin{cases} \dot{\hat{z}} = \hat{v} + (\alpha_z + \lambda_z)e_z, \\ \dot{\hat{v}} = Y(\hat{P}A_{\mathrm{m}} - \hat{Q}) + g + \alpha_z\lambda_z e \end{cases} \tag{12}$$

and

$$\begin{cases} \dot{\hat{Q}} = -k_1\sigma_z Y^{\mathrm{T}}, \\ \dot{\hat{P}} = k_2\sigma_z(A_{\mathrm{m}}Y)^{\mathrm{T}}. \end{cases} \tag{13}$$

Theorem 1 The proposed filter in (9) and (10) ensures an accurate estimation for the altitude and vertical speed such that $\hat{z}(t) \to z(t)$ and $\hat{v}(t) \to \dot{z}(t)$ as $t \to \infty$.

Proof After taking the time derivative of (12) and substituting (13) into the result, the following dynamics for $\hat{z}(t)$ can be obtained

$$\ddot{\hat{z}} = Y(\hat{P}A_{\mathrm{m}} - \hat{Q}) + g + \lambda_z\dot{e}_z + \alpha_z\sigma_z. \tag{14}$$

Let the Lyapunov function candidate $V_{\mathrm{ez}}(t) \in \mathbb{R}$ be defined as

$$V_{\mathrm{ez}} = \frac{1}{2}\sigma_z^2 + \frac{1}{2}k_2^{-1}\mathrm{tr}(\tilde{P}^{\mathrm{T}}\tilde{P}) + \frac{1}{2}k_1^{-1}\tilde{Q}^{\mathrm{T}}\tilde{Q}. \tag{15}$$

By taking the time derivative of $V_{\mathrm{ez}}(t)$ and substituting (8), (11) and (14) into the result, it can be obtained that

$$\begin{aligned} \dot{V}_{\mathrm{ez}} = & \sum_{i=1}^{3}\sum_{j=1}^{3}\tilde{p}_{ij}(\sigma_z y_i a_j - k_2^{-1}\dot{\hat{p}}_{ij}) \\ & - \tilde{Q}^{\mathrm{T}}(\sigma_z Y^{\mathrm{T}} + k_1^{-1}\dot{\hat{Q}}) - \alpha_z\sigma_z^2 \end{aligned} \tag{16}$$

considering that P, $A_{\rm m}$ and Y in (15) can be denoted by $P = \{p_{ij}\}_{3\times3}$, $Y = \{y_i\}_{1\times3}$, and $A_{\rm m} = \{a_j\}_{3\times1}$. By substituting (13) into (16), it can be obtained that

$$\dot{V}_{\rm ez} = -\alpha_z\sigma_z^2. \tag{17}$$

From (17) and (15), it is not difficult to show that $\sigma_z(t)$ converges to zero asymptotically. Recalling that $\sigma_z = \dot{e}_z + \lambda_z e_z$ with λ_z being a positive constant, then it can be shown that $e_z(t)$, $\dot{e}_z(t) \to 0$ as $t \to \infty$. Thus, it can be shown that $\hat{z}(t) \to z(t)$ and $\dot{\hat{z}}(t) \to \dot{z}(t)$ as $t \to \infty$ via (11). Finally, since $e_z(t) \to 0$ as $t \to 0$, we know that $\hat{v}(t) \to \dot{z}(t)$ as $t \to \infty$ based on the first entry of (12). □

4 Control development

This section presents the control design procedure for attitude angles and altitude position of the quadrotor under modeling uncertainties and unknown external disturbances.

4.1 Design of the attitude controller

A modified backstepping method is combined with the adaptive super-twisting algorithm to formulate the proposed control strategy. Before presenting the control laws, we introduce the following error signals:

$$\begin{cases} e_1 = \eta_{\rm d} - \eta, \\ e_2 = \Phi^{-1}(\eta)(\dot{\eta}_{\rm d} - \dot{\eta}), \end{cases} \tag{18}$$

where $\eta_{\rm d}(t) \in \mathbb{R}^3$ denotes the desired attitude trajectory vector. The stabilization of e_1 can be obtained by introducing a virtual control input for e_2 as follows:

$$e_{2\rm d} = -\Phi^{-1}(\eta)Ke_1, \tag{19}$$

where $K = {\rm diag}\{k_i\} \in \mathbb{R}^{3\times3}$ with $k_i > 0, i = \phi, \theta, \psi$ represent a gain matrix. By defining $\sigma = e_{2\rm d} - e_2$, the time derivative of (18) can be obtained as

$$\begin{cases} \dot{e}_1 = -Ke_1 - \Phi(\eta)\sigma, \\ \dot{\sigma} = J^{-1}(\tau + d) + \dot{e}_{2\rm d} - c. \end{cases} \tag{20}$$

It is worth noting that if $\sigma = 0$, then e_1 converges asymptotically to zero. Our control objective is to force σ to stay in a bounded domain, and, therefore, e_1 is also bounded in a domain.

The attitude controller is designed as follows:

$$\begin{cases} \tau = J(-\alpha|\sigma|^{\frac{1}{2}}{\rm sgn}\,\sigma - \dot{e}_{2\rm d} + c) + J(\nu + H), \\ \dot{\nu} = -\dfrac{\beta}{2}{\rm sgn}\,\sigma + \Pi, \end{cases} \tag{21}$$

where α and β denote some diagonal positive-definite adaptive gain matrixes such that $\alpha = {\rm diag}\{\alpha_i\}$ and $\beta = {\rm diag}\{\beta_i\}$ for $(i = \phi, \theta, \psi)$, ${\rm sgn}(\cdot)$ denotes the standard signum function. The gains α_i and β_i have the following adaptive laws

$$\dot{\alpha}_i = \begin{cases} \sqrt{\gamma_{i1}}{\rm sgn}(|\sigma_i| - \mu_i), & \alpha_i > \alpha_{\rm im}, \\ p_i, & \alpha_i \leqslant \alpha_{\rm im}, \end{cases} \tag{22}$$

$$\beta_i = \varepsilon_i\alpha_i, \tag{23}$$

where ε_i, γ_{i1}, μ_i and p_i are some positive constants. The parameter $\alpha_{\rm im}$ represents an arbitrary small positive constant which is used as the switching threshold value. In (21), the auxiliary function vectors $\Pi \in \mathbb{R}^{3\times1}$ and $H \in \mathbb{R}^{3\times1}$ are defined as follows:

$$\Pi_i = \begin{cases} \varepsilon_i K(e_{1i}\Phi_i(\eta)\sigma)/2\lambda_i|\sigma_i|^{\frac{1}{2}}{\rm sgn}\,\sigma_i, & |\sigma_i| > \mu_i, \\ 0, & |\sigma_i| \leqslant \mu_i, \end{cases} \tag{24}$$

$$h_i = \frac{2}{\varepsilon_i}|\sigma_i|^{\frac{1}{2}}\Pi_i, \tag{25}$$

where the defined function $K(x) = 0$ for $x \geqslant 0$ and $K(x) = x$ for $x < 0$, e_{1i} denotes the ith element of e_1 and $\Phi_i(\eta)$ represents the ith row of $\Phi(\eta)$.

The main stability result of the adaptive attitude controller proposed in (21) is stated by the following theorem.

Theorem 2 The proposed attitude controller in (21) can drive $e_1(t)$ and its time derivative $\dot{e}_1(t)$ to the domain W in finite time where W is defined as

$$W = \{e_1, \dot{e}_1 : \|e_1\|_\infty \leqslant \zeta_1, \|\dot{e}_1\|_\infty \leqslant \zeta_2\} \tag{26}$$

with ζ_1 and ζ_2 being some positive constants.

Proof By substituting from (21) and defining $\omega = \nu + J^{-1}d = \{\omega_i\}_{3\times1}$, the closed-loop system dynamics (20) can be rewritten as follows:

$$\begin{cases} \dot{e}_1 = -Ke_1 - \Phi(\eta)\sigma, \\ \dot{\sigma} = -\alpha|\sigma|^{\frac{1}{2}}{\rm sgn}\,\sigma + \omega + H, \\ \dot{\omega} = -\dfrac{\beta}{2}{\rm sgn}\,\sigma + \dfrac{{\rm d}(J^{-1}d)}{{\rm d}t} + \Pi. \end{cases} \tag{27}$$

□

To facilitate Lyapunov based stability analysis, we will present the dynamics listed in (27) into a state-space form. To this end, the following state vector is introduced

$$x_i = [x_{i1}\ \ x_{i2}]^{\mathrm{T}} = [|\sigma_i|^{\frac{1}{2}}\operatorname{sgn}\sigma_i\ \ \omega_i]^{\mathrm{T}}, \tag{28}$$

where σ_i and ω_i denote the ith element of σ and ω, respectively. Taking the time derivative of x_i, it can be obtained that

$$\begin{cases}\dot{x}_{i1} = \dfrac{1}{2|x_{i1}|}(-\alpha_i x_{i1} + x_{i2} + h_i),\\ \dot{x}_{i2} = -\dfrac{\beta_i}{2|x_{i1}|}x_{i1} + D_i + \Pi_i,\end{cases} \tag{29}$$

where $D_i = \dfrac{\mathrm{d}(J_i^{-1}d_i)}{\mathrm{d}t}$. Due to Assumption 1, we can have the upper bound of D_i as $|D_i| \leqslant \delta_3$ where $\delta_3 = \dfrac{1}{2}\max\limits_{i=\phi,\theta,\psi}\{\dfrac{1}{J_i}\}\delta_2$ with δ_2 being defined in Assumption 2. Hence, we have

$$D_i = \frac{\rho_i}{2}\operatorname{sgn}\sigma_i = \frac{\rho_i}{2}\frac{x_{i1}}{|x_{i1}|}, \tag{30}$$

where ρ_i is some bounded functions that $0 \leqslant |\rho_i| \leqslant 2\delta_3$. Substituting from (30), (29) can be rewritten in a vector-matrix format

$$\dot{x}_i = A_i x_i + B_i, \tag{31}$$

where

$$A_i = \frac{1}{2|x_{i1}|}\begin{bmatrix} -\alpha_i & 1\\ -\beta_i + \rho_i & 0\end{bmatrix} \tag{32}$$

and

$$B_i = \begin{bmatrix} \dfrac{h_i}{2|x_{i1}|}\\ \Pi_i\end{bmatrix}. \tag{33}$$

Note that if $x_{i1} \to 0$, then $\sigma_i \to 0$ (for $i = \phi, \theta, \psi$), since $\Phi_i(\eta)$ is bounded (due to Assumption 3), then $\Phi_i(\eta)\sigma \to 0$. In view of (27), the convergence of e_{1i} is guaranteed as well. Thus, the Lyapunov's direct method is employed for the convergence of x_i. After that, the stability analysis for e_{1i} is presented. The Lyapunov function candidate V_i is defined as

$$V_i = V_{i1} + V_{i2}, \tag{34}$$

where $V_{i1} = \dfrac{1}{2}e_{1i}^2$ and the function V_{i2} is defined as

$$V_{i2} = V_{io} + \frac{1}{\gamma_{i1}}(\alpha_i - \alpha_i^*)^2 + \frac{1}{\gamma_{i2}}(\beta_i - \beta_i^*)^2 \tag{35}$$

with α_i^*, β_i^* being some positive constants. The non-negative function V_{io} in (35) is defined as $V_{io} := x_i^{\mathrm{T}}P_i x_i$ where

$$P_i = \begin{bmatrix} \lambda_i + \varepsilon_i^2 & -\varepsilon_i\\ -\varepsilon_i & 1\end{bmatrix} \tag{36}$$

is positive definite if $\lambda_i > 0$ and ε_i are real number. Substituting from (31), the time derivative of V_{io} can be obtained as

$$\dot{V}_{io} = x_i^{\mathrm{T}}(A_i^{\mathrm{T}}P_i + P_i A_i)x_i + 2x_i^{\mathrm{T}}P_i B_i. \tag{37}$$

By substituting from (25), (33), (36), $\dot{V}_{io}$ in (37) can be rewritten as

$$\dot{V}_{io} = -\frac{1}{2|x_{i1}|}x_i^{\mathrm{T}}Q_i x_i + \frac{2\lambda_i}{\varepsilon_i}x_{i1}\Pi_i, \tag{38}$$

where

$$Q_i = \begin{bmatrix} q_{11}^i & q_{12}^i\\ q_{21}^i & 2\varepsilon_i\end{bmatrix} \tag{39}$$

with

$$\begin{cases} q_{11}^i = 2\alpha_i(\varepsilon_i^2 + \lambda_i) - 2\varepsilon_i(\beta_i - \rho_i),\\ q_{21}^i = q_{12}^i = -\varepsilon_i^2 - \alpha_i\varepsilon_i + \beta_i - \lambda_i - \rho_i.\end{cases} \tag{40}$$

Substituting from (23), The matrix Q_i will be positive definite with a minimal eigenvalue $\lambda_{\min}(Q_i) \geqslant \varepsilon_i$ if

$$\alpha_i > \frac{-\varepsilon_i(4\delta_3 + 1)}{2\lambda_i} + \frac{(2\delta_3 + \lambda_i + \varepsilon_i^2)^2}{6\varepsilon_i\lambda_i}. \tag{41}$$

The right hand side of (41) is a bounded unknown constant. If we assume (41) holds, then from (38), we can obtain

$$\dot{V}_{io} \leqslant -r_i V_{io}^{\frac{1}{2}} + \frac{2\lambda_i}{\varepsilon_i}x_{i1}\Pi, \tag{42}$$

where $r_i = \varepsilon_i\lambda_{\min}^{\frac{1}{2}}(P_i)/2\lambda_{\max}(P_i)$ (see proof in [17]).

Taking the time derivative of V_{i1} and substituting from (27) yields

$$\dot{V}_{i1} = -2k_i V_{i1} - e_{1i}\Phi_i(\eta)\sigma. \tag{43}$$

By substituting from (35), (42), (43), $\dot{V}_i$ can be rewritten as follows:

$$\begin{aligned}\dot{V}_i =& \dot{V}_{io} + \dot{V}_{i1} + \frac{1}{\gamma_{i1}}\varepsilon_\alpha^i\dot{\alpha}_i + \frac{1}{\gamma_{i2}}\varepsilon_\beta^i\dot{\beta}_i \\ \leqslant& -2k_iV_{i1} - r_iV_{io}^{\frac{1}{2}} - \frac{|\varepsilon_\alpha^i|}{\sqrt{\gamma_{i1}}} - \frac{|\varepsilon_\beta^i|}{\sqrt{\gamma_{i2}}} \\ &+ \frac{1}{\gamma_{i1}}\varepsilon_\alpha^i\dot{\alpha}_i + \frac{1}{\gamma_{i2}}\varepsilon_\beta^i\dot{\beta}_i + \frac{|\varepsilon_\alpha^i|}{\sqrt{\gamma_{i1}}} + \frac{|\varepsilon_\beta^i|}{\sqrt{\gamma_{i2}}} + F_i \\ \leqslant& -2k_iV_{i1} - \eta_i\sqrt{V_{i2}} + \chi_i,\end{aligned} \tag{44}$$

where $\varepsilon_\alpha^i = \alpha_i - \alpha_i^*$, $\varepsilon_\beta^i = \beta_i - \beta_i^*$, $F_i = \dfrac{2\lambda_i}{\varepsilon_i}x_{i1}\Pi_i - e_{1i}\Phi_i(\eta)\sigma$ and $\chi_i = -|\varepsilon_\alpha^i|\Big(\dfrac{1}{\gamma_{i1}}\dot{\alpha}_i - \dfrac{1}{\sqrt{\gamma_{i1}}}\Big) - |\varepsilon_\beta^i|\Big(\dfrac{1}{\gamma_{i2}}\dot{\beta}_i - \dfrac{1}{\sqrt{\gamma_{i2}}}\Big) + F_i$.

The following two cases will be considered to obtained the result listed in Theorem 2.

Case 1 Suppose that $|\sigma_i| > \mu_i$ and $\alpha_i(t) > \alpha_{im}$, $\forall t \geqslant 0$. Then, in view of (22), we have

$$\dot{\alpha}_i = \sqrt{\gamma_{i1}}. \tag{45}$$

Selecting $\gamma_{i2} = \varepsilon_i^2\gamma_{i1}$ and differentiating (23), we obtain

$$\dot{\beta}_i = \varepsilon_i\dot{\alpha}_i = \sqrt{\gamma_{i2}}. \tag{46}$$

Substituting from (24), F_i is computed such that $F_i \leqslant 0$. Substituting from (45), (46), the first two terms on the right hand side of (44) are cancelled. Thus, it is easy to have $\chi_i \leqslant 0$ and

$$\dot{V}_i \leqslant -2k_iV_{i1} - \eta_i\sqrt{V_{i2}}. \tag{47}$$

As soon as (41) is satisfied, σ_i converges to the domain $|\sigma_i| \leqslant \mu_i$ in finite time t_{Fi} (see Lemma 1 in the appendix).

Case 2 Suppose that $|\sigma_i| < \mu_i$, then the control gain $\alpha_i(t)$ is reducing in accordance with (22) such that

$$\dot{\alpha}_i = \begin{cases} -\sqrt{\gamma_{i1}}, & \alpha_i > \alpha_{im}, \\ p_i, & \alpha_i \leqslant \alpha_{im}. \end{cases} \tag{48}$$

Note the term F_i included in χ_i becomes $-e_{1i}\Phi_i(\eta)\sigma$, and in view of the structure of χ_i when substituting from (48), χ_i becomes sign indefinite as well as $\dot{V}_i$ which comprises χ_i.

Thus, the above two cases for $\dot{V}_i$ ensure that after a finite time t_{Fi}, σ_i will always stay in a domain $|\sigma_i| \leqslant \rho_i$ with $\rho_i > \mu_i$ (See the discussion presented in [17]).

In other words, σ converges to the domain W_σ in finite time $t_F = \max\{t_{Fi}\}$ (for $i = \phi, \theta, \psi$) where

$$W_\sigma = \{\sigma : \|\sigma\|_\infty \leqslant \rho\} \tag{49}$$

with $\|\cdot\|_\infty$ denoting infinity norm, ρ being defined as $\rho = \max\{\rho_i\}$ (for $i = \phi, \theta, \psi$).

Notice that $\Phi(\eta) = \{\varphi_i\}_{3\times3}$ is bounded due to Assumption 3 such that $|\varphi_i| \leqslant \xi$, $\xi > 0$, we have the second term on the right side of (27) bounded such that $|\Phi_i(\eta)\sigma| \leqslant 3\xi\rho$. Then, according to (27), we can conclude that e_{1i} converges to the domain $|e_{1i}| \leqslant 6\xi\rho/k_i$ as well as its time derivative $\dot{e}_{1i}$ to the domain $|\dot{e}_{1i}| \leqslant 9\xi\rho$ in finite time t_{Hi} (see Lemma 2 in the appendix). In other words, the finite time convergence of e_1 and its time derivative $\dot{\boldsymbol{e}}_1$ to the domain W is guaranteed where

$$W = \{\boldsymbol{e}_1, \dot{\boldsymbol{e}}_1 : \|\boldsymbol{e}_1\|_\infty \leqslant \zeta_1, \|\dot{\boldsymbol{e}}_1\|_\infty \leqslant \zeta_2\}, \tag{50}$$

where $\zeta_1 = 6\xi\rho/k$, $k = \min\{k_i\}$ for $i = \phi, \theta, \psi$, and $\zeta_2 = 9\xi\rho$.

4.2 Design of the altitude controller

To facilitate the control objective for the altitude channel of the quadrotor, the altitude tracking error signal $e_z(t)$ and its sliding mode manifold $\sigma_z(t)$ are introduced as follows:

$$\begin{cases} e_z = z_d - z, \\ \sigma_z = \dot{e}_z + \lambda e_z, \end{cases} \tag{51}$$

where λ is a positive gain.

By taking the time derivative of $\sigma_z(t)$ and substituting (4) into the result, it can be obtained that

$$\dot{\sigma}_z = u_t\cos\phi\cos\theta/m - d_t + c_z, \tag{52}$$

where $c_z = \ddot{z}_d - g + \lambda\dot{e}_z$. Similar as the control development for the attitude controller $\tau(t)$, the altitude controller is designed as follows:

$$\begin{cases} u_t = \dfrac{m}{\cos\phi\cos\theta}(-\alpha_z|\sigma_z|^{\frac{1}{2}}\operatorname{sgn}\sigma_z - c_z + \nu_z), \\ \dot{\nu}_z = -\dfrac{\beta_z}{2}\operatorname{sgn}\sigma_z, \end{cases} \tag{53}$$

where α_z and β_z are the adaptive gains with the following updating laws:

$$\dot{\alpha}_z = \begin{cases} \sqrt{\gamma_{z1}}\operatorname{sgn}(|\sigma_z| - \mu_z), & \alpha_z > \alpha_{zm}, \\ p_z, & \alpha_z \leqslant \alpha_{zm}, \end{cases} \tag{54}$$

$$\beta_z = \varepsilon_z \alpha_z \tag{55}$$

with ε_z, γ_{z1}, μ_z and p_z being some positive constants. The parameter α_{zm} denotes an arbitrary small positive constant which is employed as the switching threshold value.

The main stability result of the adaptive altitude controller proposed in (53) is stated by the following theorem.

Theorem 3 The proposed controller can drive $e_z(t)$ and its time derivative $\dot{e}_{z1}$ to the domain W_z in finite time where W_z is defined as follows:

$$W_z = \{e_z, \dot{e}_z : \|e_z\|_\infty \leqslant \zeta_{z1}, \|\dot{e}_z\|_\infty \leqslant \zeta_{z2}\} \tag{56}$$

with ζ_{z1} and ζ_{z2} being some positive constants.

Proof The proof of Theorem 3 can be completed by the following the similar steps for the proof of Theorem 2.

5 Experimental results

In this section, the proposed control strategy in Sections 3 and 4 is implemented on a self-built quadrotor helicopter flying testbed in an indoor environment to validate its performance as shown in Fig. 2. The physical parameters of the quadrotor helicopter are listed in Table 1. The control loop runs at a frequency of 1 kHz to ensure high performance of real-time response.

The nonlinear complementary filter proposed in Section 3 provides the altitude estimation information for the closed-loop operation. Its reliability is validated by a comparison between the estimated value and true value as shown in Fig. 3. A OptiTrack motion capture system is employed to provide ground truth values for the quadrotor helicopter during the flighting test, these ground truth information is used only for the purpose of comparison, but not utilized in the closed-loop control. In Fig. 3, $\hat{z}(t)$ and $\hat{v}(t)$ represent the altitude estimation and vertical velocity estimation values obtained from the nonlinear complementary filter in (12), $z_r(t)$ and $v_r(t)$ represent the real altitude and vertical velocity values obtained from the motion capture system. From Fig. 3, it can be seen that the maximum estimation error for the quadrotor's altitude position is less than ±0.2 m, and the maximum estimation error for the quadrotor's vertical velocity is less than ±0.18 m/s. Considering about the fact that the accuracy for the direct altitude measurement from the onboard barometer is about ±0.5 m, the nonlinear complementary filter proposed in (12) has achieved a good accuracy for the altitude position and vertical velocity measurement.

Fig. 2 Quadrotor helicopter flight testbed.

Table 1 Parameters for the quadrotor helicopter testbed.

Parameter	Description	Value	Units
m	Mass	0.944	kg
J_ϕ	Roll inertia	6.6×10^{-3}	$\mathrm{kg \cdot m^2}$
J_θ	Pitch inertia	6.6×10^{-3}	$\mathrm{kg \cdot m^2}$
J_ψ	Yaw inertia	1.19×10^{-2}	$\mathrm{kg \cdot m^2}$

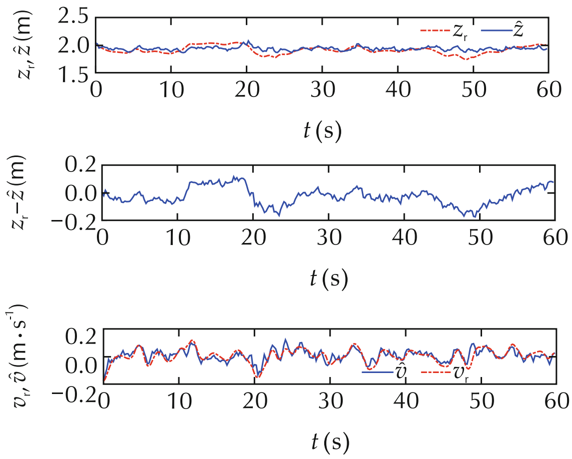

Fig. 3 Comparision between the estimation values ($z(t)$, $v(t)$) and real values ($z_r(t)$, $v_r(t)$).

To validate the performance for the attitude and altitude controllers proposed in Section 4, a stabilization flight test is implemented on the quadrotor helicopter testbed. The control objective is to stabilize the quadrotor's attitude angle ($\phi(t)$, $\theta(t)$, $\psi(t)$) to be $[\phi_d\ \ \theta_d\ \ \psi_d]^T = [0\ \ 0\ \ 0]^T$, and the quadrotor's altitude $z(t)$ to be some desired value as $z_d = 1.94$ m. The quadrotor is first taken off manually to a proper position, and then the pilot flips the switcher on the RC controller to turn the quadrotor into automatic stabilizing control procedure, and the automatic control period lasts about 60 seconds. The control gains for attitude and altitude controllers are selected as follows for the best control performance:

$$\begin{cases} k_{\phi,\theta} = 4.5, \ \ k_{\psi} = 4.8, \ \ \lambda_{\phi,\theta} = 0.013, \ \ \lambda_{\psi} = 0.038, \\ \lambda_z = 1.3, \ \ \mu_{\phi,\theta} = 0.064, \ \ \mu_{\psi} = 0.058, \ \ \mu_z = 0.02, \\ \alpha_{\phi m} = 7.90, \ \ \alpha_{\theta m} = 7.90, \ \ \alpha_{\psi m} = 5.85, \ \ \alpha_{zm} = 0.1, \\ \varepsilon_{\phi,\theta,\psi} = 0.396, \ \ \gamma_{\phi,\theta} = 9.24, \ \ \gamma_{\psi} = 8.41, \ \ \gamma_z = 1.59. \end{cases} \tag{57}$$

Fig. 4 shows the actual attitude response and its desired value. It can be seen that maximum stabilization error for the roll channel is about ±1.1°, the maximum stabilization error for the pitch channel is about ±0.8°, the maximum stabilization error for the yaw channel is about ±1.2°, thus the proposed control strategy has shown good attitude control performance. The stabilization performance for the altitude channel is shown in Fig. 5 where $\hat{z}(t)$ is used as the closed-loop response for the quadrotor's altitude position. It can be seen that the maximum altitude stabilization error is about ±0.12 m, and the maximum vertical velocity stabilization error is less than ±0.12 m/s, thus the proposed control strategy has achieve good altitude control performance for the quadrotor. From both Fig. 4 and Fig. 5, it can be seen that the quadrotor's outputs ($\phi(t)$, $\theta(t)$, $\psi(t)$, $z(t)$) converge to their desired values very quickly. The adaptive control gains (α_{ϕ}, α_{θ}, α_{ψ}, α_z) designed in (22) and (54) are depicted in Fig. 6, they are all bounded. The control inputs (τ_{ϕ}, τ_{θ}, τ_{ψ}, u_t) are illustrated in Fig. 7, they all stay with some reasonable values.

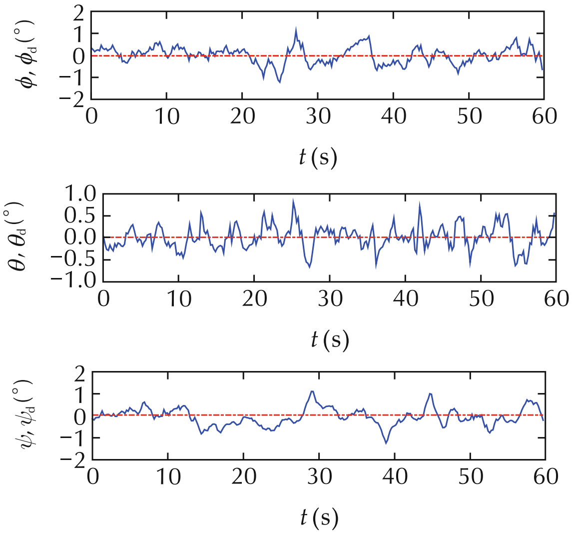

Fig. 4 Actual attitude angles ($\phi(t)$, $\theta(t)$, $\psi(t)$) and their desired values.

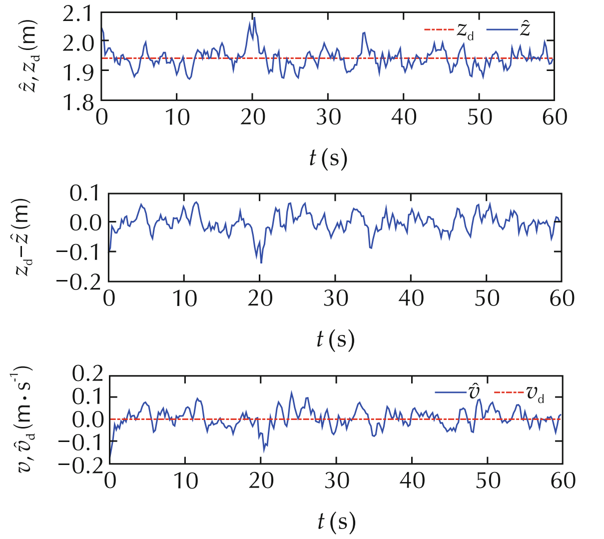

Fig. 5 Actural altitude $\hat{z}(t)$, vertical velocity $\hat{v}(t)$ and their desired value (z_{d}, v_{d}).

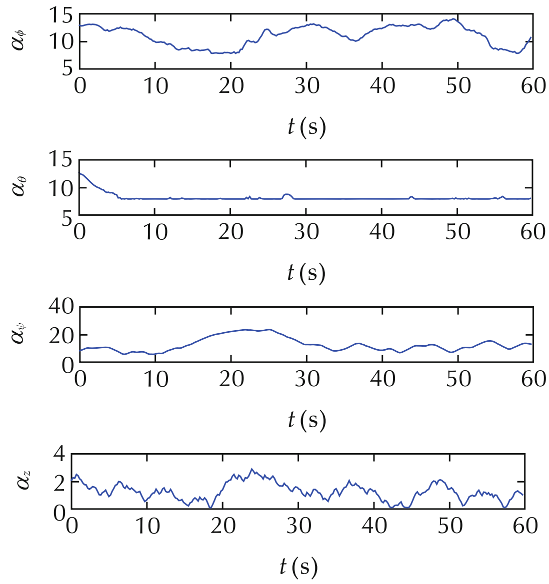

Fig. 6 Adaptive gains (α_{ϕ}, α_{θ}, α_{ψ}, α_z).

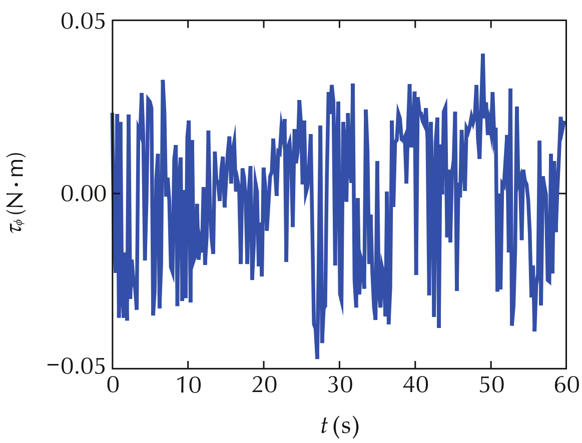

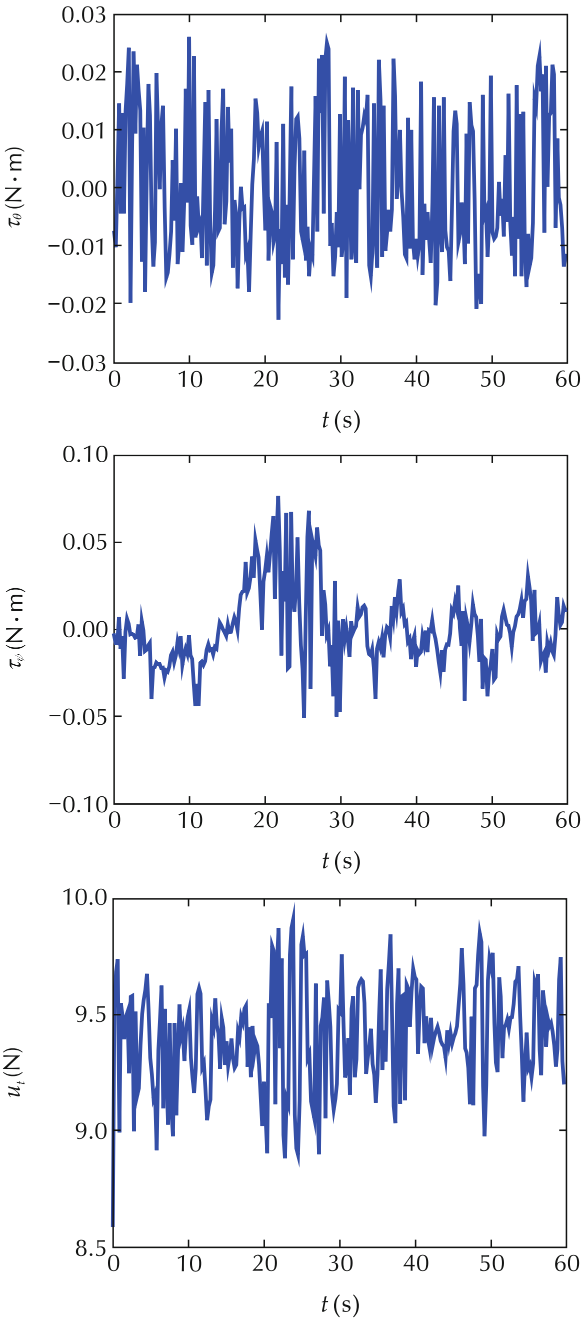

Fig. 7 Control inputs (τ_ϕ, τ_θ, τ_ψ, u_t).

6 Conclusions

This paper considers the control problem for a quadrotor helicopter which is subjected to modeling uncertainties and unknown nonvanishing external disturbances. The quadrotor's roll angle, pitch angle, yaw angle, and altitude are selected as the system's outputs. To improve the measurement accuracy for the altitude channel, a nonlinear complementary is developed and its convergence is proven. Based on the adaptive super-twisting scheme, a nonlinear adaptive controller for the quadrotor is developed and its finite time convergence is proven via the Lyapunov-based stability analysis. Real-time flight experimental results are presented to validate the performance of the proposed control strategy. Future work will focus on developing position controller together with the attitude controller for the quadrotor helicopter to achieve finite time convergence of the position tracking error under effects of parametric uncertainties and external disturbances.

References

[1] Y. Du, J. Fang, C. Miao. Frequency domain system identification of an unmanned helicopter based on adaptive genetic algorithm. *IEEE Transactions on Industrial Electronics*, 2014, 61(2): 870 – 881.

[2] M. D. Hua, T. Hamel, P. Morin, et al. Introduction to feedback control of underactuated VTOL vehicles: a review of basic control design ideas and principles. *IEEE Control System Magzine*, 2013, 33(1): 61 – 75.

[3] K. Alexis, G. Nikolakopoulos, A. Tzes. Model predictive quadrotor control: attitude, altitude and position experimental studies. *IET Control Theory and Applications*, 2012, 6(12): 1812 – 1827.

[4] B. Zhao, B. Xian, Y. Zhang, et al. Nonlinear robust adaptive tracking control of a quadrotor UAV via immersion and invariance methodology. *IEEE Transactions on Industrial Electronics*, 2015, 62(5): 2891 – 2902.

[5] B. Xian, X. Zhang, S. Yang. Nonlinear controller design for an unmanned aerical vehicle with a slung-load. *Control Theory & Applications*, 2016, 33(3): 273 – 279 (in Chinese).

[6] W. Hao, B. Xian. Nonlinear fault tolerant control design for quadrotor unmanned aerial vehicle attitude system. *Control Theory & Applications*, 2015, 32(11): 1457 – 1463 (in Chinese).

[7] X. Zhang, B. Xian, B. Zhao, et al. Autonomous flight control of a nano quadrotor helicopter in a GPS-denied environment using on-board vision. *IEEE Transactions on Industrial Electronics*, 2015, 62(10): 6392 – 6403.

[8] J. Toledo, L. Acosta, D. Perea, et al. Stability and performance analysis of unmanned aerial vehicles: quadrotor against hexrotor. *IET Control Theory and Applications*, 2015, 9(8): 1190 – 1196.

[9] G. V. Raffo, M. G.Ortega, F. R. Rubio. An integral predictive/nonlinear H_∞ control structure for a quadrotor helicopter. *Automatica*, 2010, 46(1): 29 – 39.

[10] R. Zhang, Q. Quan, K. Y. Cai. Attitude control of a quadrotor aircraft subject to a class of time-varying disturbances. *IET Control Theory and Applications*, 2011, 5(1): 1140 – 1146.

[11] H. Ramirez-Rodriguez, V. Parra-Vega, A. Sanchez-Orta, et al. Robust backstepping control based on integral sliding modes for tracking of quadrotors. *Journal of Intelligent and Robotic Systems*, 2014, 73(1/4): 51 – 66.

[12] H. Liu, Y. Bai, G. Lu, et al. Robust motion control of uncertain

quadrotors. *Journal of the Franklin Institute*, 2014, 351(12): 5494 – 5510.

[13] H. Liu, Y. Bai, G. Lu, et al. Robust tracking control of a quadrotor helicopter. *Journal of Intelligent and Robotic Systems*, 2014, 75(3/4): 595 – 608.

[14] B. J. Bialy, J. Klotz, K. Brink, et al. Lyapunov-based robust adaptive control of a quadrotor UAV in the presence of modeling uncertainties. *Proceedings of the American Control Conference*, Washington: IEEE, 2013: 13 – 18.

[15] Y. Yu, X. Ding, J. Zhu. Attitude tracking control of a quadrotor UAV in the exponential coordinates. *Journal of the Franklin Institute*, 2013, 350(8): 2044 – 2068.

[16] L. Derafaa, A. Benallegueb, L. Fridman. Super twisting controlal gorithm for the attitude tracking of a four rotors UAV. *Journal of the Franklin Institute*, 2012, 349(2): 658 – 699.

[17] Y. Shtesse, M. Taleb, F. Plestan. A novel adaptive-gain supertwisting sliding mode controller: methodology and application. *Automatica*, 2012, 48(5): 759 – 769.

[18] F. Kendoul, Z. Yu, K. Nonami. Guidance and nonlinear control system for autonomous flight of minirotorcraft unmanned aerial vehicles. *Journal of Field Robotics*, 2010, 27(3): 311 – 334.

[19] B. Xian, C. Diao, B. Zhao, et al. Nonlinear robust output feedback tracking control of a quadrotor UAV using quaternion representation. *Nonlinear Dynamics*, 2015, 79(4): 2735 – 2752.

[20] I. Gonzalez, S. Salazar, R. Lozano, et al. Real-time altitude robust controller for a quad-rotor aircraft using sliding-mode control technique. *Proceeding of the International Conference on Unmanned Aircraft Systems*, Atlanta: IEEE, 2013: 650 – 659.

[21] J. Hu, H. Zhang. Immersion and invariance based command-filtered adaptive backstepping control of VTOL vehicles. *Automatica*, 2013, 49(7): 2160 – 2167.

[22] R. Mahony, T. Hamel, J. M. Pflimlin. Nonlinear complementary filters on the special orthogonal group. *IEEE Transactions on Automatic Control,* 2008, 53(5): 1203 – 1218.

Appendix

Lemma 1 As soon as (41) is fulfilled in finite time t_{0i}, $\sigma_i(t)$ converges to the domain $|\sigma_i| \leqslant \mu_i$ in finite time $t_{\mathrm{F}i}$.

Proof In view of (34), (35), it is easy to obtain

$$V_i \geqslant V_{i2} \geqslant x_i^{\mathrm{T}} P_i x_i \geqslant \lambda_{\min}(P_i)\|x_i\|^2 \geqslant \lambda_{\min}(P_i)|\sigma_i|, \tag{a1}$$

Now, all we need to do is to find $t_{\mathrm{F}i}$ that ensures $V_i(t) \leqslant \lambda_{\min}(P_i)\mu_i$, $\forall t \geqslant t_{\mathrm{F}i} + t_{0i}$. Note that the (41) is satisfied and Case 1 holds, in view of (47) we have the time derivative of V_i

$$\dot{V}_i \leqslant -c_i(V_{i1} + \sqrt{V_{i2}}), \tag{a2}$$

where $c_i = \min\{2k_i, \eta_i\}$. The following two cases are investigated.

Case a) $V_{i1} \geqslant 1$ or $V_{i2} \geqslant \dfrac{1}{4}$, we can derive

$$V_{i1} + \sqrt{V_{i2}} \geqslant \sqrt{V_{i1} + V_{i2}}, \tag{a3}$$

then finite time convergence of V_i is guaranteed such that

$$\dot{V}_i \leqslant -c_i\sqrt{V_i}. \tag{a4}$$

Case b) $V_{i1} < 1$ and $V_{i2} < \dfrac{1}{4}$, we have

$$V_{i1} + \sqrt{V_{i2}} \geqslant V_{i1} + V_{i2}, \tag{a5}$$

then exponential convergence of V_i is guaranteed such that

$$\dot{V}_i \leqslant -c_i V_i. \tag{a6}$$

It can be observed that Case a) holds when $V_i \geqslant \dfrac{5}{4}$ and Case b) holds when $V_i < \dfrac{1}{4}$. When $1 < V_i < \dfrac{5}{4}$, either of the two cases holds so that

$$\dot{V}_i \leqslant -c_i \min\{\sqrt{V_i}, V_i\} = -c_i\sqrt{V_i}, \tag{a7}$$

whereas we have $\dot{V}_i \leqslant -c_i V_i$ when $\dfrac{1}{4} \leqslant V_i \leqslant 1$. Thus, V_i decreases from its initial condition $V_i(t_{0i})$ with decreasing rate satisfying

$$\dot{V}_i \leqslant \begin{cases} -c_i\sqrt{V_i}, & V_i > 1, \\ -c_i V_i, & V_i \leqslant 1, \end{cases} \tag{a8}$$

and converges to the domain $|V_i| \leqslant \lambda_{\min}(P_i)\mu_i$ with convergence time $t_{\mathrm{F}i}$ satisfying

$$t_{\mathrm{F}i} \leqslant \frac{2V_i^{\frac{1}{2}}(t_{0i})}{c_i} + \frac{1}{c_i}\ln(\frac{V_i(t_{0i})}{\lambda_{\min}(P_i)\mu_i}), \tag{a9}$$

Then, in view of (a1), $|\sigma_i(t)| \leqslant \mu_i$ is guaranteed for $\forall t \geqslant t_{\mathrm{F}i} + t_{0i}$. Thus the result listed in Lemma 1 is proved. □

Lemma 2 The error signal $e_{1i}(t)$ converges to the domain $|e_{1i}| \leqslant 6\xi\rho/k_i$ as well as its time derivative $\dot{e}_{1i}$ to the domain $|\dot{e}_{1i}| \leqslant 9\xi\rho/2$ in finite time $t_{\mathrm{H}i}$.

Proof Recalling (27), where the term $\Phi_i(\eta)\sigma$ is bounded such that $|\Phi_i(\eta)\sigma| \leqslant 3\xi\rho$, it is obvious that $|e_{1i}| < 3\xi\rho/k_i$, as $t \to \infty$. Now, we assume that $|e_{1i}(t_{\mathrm{F}i})| > 6\xi\rho/k_i$. In view of (27), it is easy to have $|e_{1i}(t)| \leqslant 6\xi\rho/k_i$, for $\forall t \geqslant t_{\mathrm{H}i}$, where

$$t_{\mathrm{H}i} = t_{\mathrm{F}i} + \frac{1}{k_i}\ln\frac{k_i e(t_{\mathrm{F}i}) - 3\xi\rho}{3\xi\rho}. \tag{a10}$$

Furthermore, we have the time derivative of e_{1i}

$$\begin{aligned} |\dot{e}_{1i}| &\leqslant |-k_i e_{1i} + \Phi_i(\eta\sigma)| \\ &\leqslant |-k_i e_{1i}| + |\Phi_i(\eta)\sigma| \\ &\leqslant 9\xi\rho. \end{aligned} \tag{a11}$$

Thus the result listed in Lemma 2 is proved. □

Guozhou ZHENG is a graduate student with the School of Electrical and Information Engineering, Tianjin University. His main research area is nonlinear control of quadrotor unmanned aerial vehicle. E-mail: gz_zheng@tju.edu.cn.

Bin XIAN is a professor with the School of Electrical and Information Engineering, Tianjin University. His main research area focuses on autonomous unmanned aerial vehicles, intelligent robot system, and nonlinear control. E-mail: xbin@tju.edu.cn.